Protein Expression and Purification 192 (2022) 106042

Contents lists available at ScienceDirect

Protein Expression and Purification

journal homepage: www.elsevier.com/locate/yprep

Biochemical and functional characterization of the N-terminal ubiquitin-like domain of human SHARPIN

Wenlei Ma [a], Ying Lu [b], Jing Qi [c], Yongmei Zuo [d], Chenchen Wang [a], Xiaodong Zheng [c,**], Jiafu Liu [c,*]

[a] College of Veterinary Medicine, Northeast Agricultural University, Harbin, 150030, China
[b] College of Life Sciences, Northeast Agricultural University, Harbin, 150030, China
[c] School of Basic Medical Sciences, Harbin Medical University-Daqing, Daqing, 163319, China
[d] Heilongjiang Institute of Animal Health Inspection, Harbin, 150006, China

ARTICLE INFO

Keywords:
SHARPIN
LUBAC
Ubiquitin-like
Co-expression
Biological activity

ABSTRACT

SHARPIN, an accessory subunit of the E3 ligase complex LUBAC, participates in the formation of LUBAC through the ubiquitin-like (UBL) domain located in the central region of SHARPIN and interacts with the ubiquitin-associated domain (UBA) of the catalytic subunit HOIP. However, the role of the N-terminal UBL domain of SHARPIN in stable LUBAC formation has not been clarified. In this study, the 1–127 domain, 128–309 domain, and UBL domain of SHARPIN expression vectors were constructed using the molecular biology method. Then the co-expression of SUMO fusion protein combined with SUMO protease (ULP enzyme) in *Escherichia coli* was successfully applied to improve the soluble expression of target protein. The results of circular dichroism proved that they all belong to the α+β class of proteins. The results of size exclusion chromatography showed that 128–309 domain could combine with HOIP and HOIL-1L to participate in the stability of LUBAC. Both thermal-induced and urea-induced unfolding experiment results demonstrated that the existence of the N-terminal UBL domain could make the overall structure more stable than the alone UBL domain. Biosensor experiments indicated that the existence of the N-terminal UBL domain strengthened the binding ability of the UBL domain and the UBA domain. These results were conducive to further study the structure and function of SHARPIN.

1. Introduction

SHARPIN (SHANK-associated RH domain interacting protein) originally has been identified as a SHANK (SH3 (Src homology 3) and multiple ankyrin repeat domains protein)-binding protein, containing 387-amino acids [1]. It is enriched in the postsynaptic dense region and is common in mammals including humans, mice, rats, dogs, cattle, and chimpanzees, but not found in lower organisms such as *Caenorhabditis elegans* and Drosophila. Previous studies have observed that spontaneous mutation of SHARPIN gene in mice could lead to chronic proliferative dermatitis, which is a disease characterized by skin damage and multi organ inflammation. The deficiency of immune system suggested that SHARPIN may also be related to immune and inflammatory signaling pathways [2]. Recently, the role of SHARPIN in the regulation of the immune system has been confirmed. SHARPIN acts as a novel subunit to form the linear ubiquitin chain assembly complex (LUBAC) and participates in the regulation of immune signals [3]. LUBAC participates in inflammatory and carcinogenic signaling mainly by binding linear ubiquitin chains to target proteins [4]. In addition, LUBAC also activates the NF-κB pathway by catalyzing the Met1-polyubiquitination of NEMO (IKKγ).

LUBAC is composed of three subunits: a catalytic subunit, HOIP and two accessory subunits, SHARPIN and HOIL-1L. Previous reports showed that malfunction of any of the three LUBAC subunits caused inflammation, immunodeficiency, or even death in animal models and/or humans [5]. For example, deletion of the catalytic subunit HOIP led to abnormal endothelial cell death, defective angiogenesis, and mid embryonic death (E10.5) [6]. Interestingly, mice lacking SHARPIN and HOIL-1L showed different phenotypes, although the two subunits were structurally similar. Mice expressing SHARPIN dysfunction exhibited multiple organ defects, including chronic inflammation and immunodeficiency, which may be attributed to NF-κB activation and dysfunction

* Corresponding author. Harbin Medical University-Daqing, Daqing, 163319, China.
** Corresponding author.
E-mail addresses: zhengxiaodong@hmudq.edu.cn (X. Zheng), jiafuliu@gmail.com (J. Liu).

https://doi.org/10.1016/j.pep.2021.106042
Received 1 November 2021; Received in revised form 20 December 2021; Accepted 20 December 2021
Available online 26 December 2021

of the apoptotic signaling pathway [7,8]. In contrast, HOIL-1L knockout (KO) mice did not show any significant inflammatory diseases [9]. In addition, SHARPIN could directly interact with the kindlin-1 to suppress β1-integrin activation, but the interaction of SHARPIN with integrin and HOIP was mutually exclusive [7,10]. Previous studies indicated that SHARPIN was mainly involved in the interaction with integrin and HOIP through the UBL domain (residues 206–309), but the binding sites were different [10].

Both SHARPIN and HOIL-1L contain UBL domain and Npl4 zinc finger (NZF) domain. Their amino acid sequences are highly similar [11]. However, SHARPIN uniquely has an N-terminal pleckstrin homology (PH) domain (residues 1–127) [12]. The PH domain does not appear to be used as a ligand recognition domain because it lacks many surface properties that exist in other interaction modules based on pleckstrin homologous folding. SHARPIN and HOIL-1L interact through their UBL domain with the ubiquitin-associated (UBA) domain (residues 480–639) of HOIP to maintain the stability of LUBAC [13]. In addition, LUBAC-tethering motifs(LTMs) located at the N terminal of the UBL domains of HOIL-1L (residues 1–140) and SHARPIN(residues 170–206) fold into a single globular domain to resistant dissociation and play a critical role in stabilizing trimeric LUBAC (Fig. 1) [4]. However, the role of the 128–309 domain of SHARPIN in stable LUBAC formation has remained elusive. Given the key roles played by SHARPIN in the stability of LUBAC, it is necessary to further study the biochemical and functional characterization of the 128–309 domain of SHARPIN.

In this study, the 1–127 domain, 128–309 domain, and UBL domain of SHARPIN prokaryotic expression vectors were constructed using molecular biology and structural biology methods. Then we used a new method previously studied in our laboratory that the SUMO fusion expression system combined with ULP enzyme to co-express in *Escherichia coli* to obtain the target protein [14]. Through exploring and optimizing the expression conditions of recombinant protein, affinity chromatography and gel filtration chromatography, a large number of stable and high-purity protein samples were successfully prepared. Finally, by SDS-PAGE, analytical size-exclusion chromatography and circular dichroism (CD) spectroscopy, it was further identified that the target protein obtained by using co-expression technology could be folded correctly and used for functional research. Meanwhile, the functional relationship between SHARPIN with HOIP and HOIL-1L was also clarified. Both thermal-induced and urea-induced unfolding results demonstrated that the 1–127 domain was more stable than the 128–309 domain and UBL domain. Biosensor experiments indicated that the existence of the 128–206 domain strengthened the binding and resisted dissociation ability between the UBL domain of SHARPIN and the UBA domain of HOIP. These results would further benefit the research on the structure and function of SHARPIN.

2. Materials and methods

The 1–127 domain, 128–309 domain, and UBL domain of SHARPIN were cloned into pET-SUMO expression vector using *Bam HI* and *Hind* III restriction sites. The plasmid construction of HOIP's UBA domain, HOIL-$1L^{1-140}$ domain and ULP enzyme, target protein expression and purification, secondary structure determination, thermal and urea induced unfolding, and analytical size-exclusion chromatography experiments were conducted as described previously [14].

In addition, the difference in binding affinity of HOIP UBA domain to 128–309 domain, UBL domain, 128–309 domain/HOIL-$1L^{1-140}$ domain complex, and that of 128–309 domain to HOIL-$1L^{1-140}$ domain were determined using Amine Reative 2nd Generation (AR2G) biosensors in the Octet Red 96 instrument. As described above, the gradient concentration of UBA domain, HOIL-$1L^{1-140}$ domain, 128–309 domain and UBL domain were prepared in buffer A (25 Mm Tris-HCl, 100 mM NaCl, pH 7.5). AR2G tips were pre-wetted in buffer A for 10 min before use, and the 96-well black plates utilized in the Octet were filled with 200 μL of sample or buffer per well and agitated at 1000 rpm. After loading the UBA domain on the AR2G biosensor, flush it with buffer A for 120 s, and then transfer it to the wells containing the samples in buffer A, i.e. 128-309 domain, UBL domain, and 128–309 domain/HOIL-$1L^{1-140}$ domain complex. The binding affinity of 128–309 domain to HOIL-$1L^{1-140}$ domain was also measured using the same method. We measured the association and dissociation for 10 min, respectively. The kinetic parameters and affinities were calculated from a non-linear global fit of the data between the four proteins, using Octet Data Analysis software version 7.0 (ForteBio Inc., Menlo Park, CA, USA).

3. Results

3.1. Construction of recombinant plasmid

The construction of co-expression system was conducted as described previously (Fig. 2A) [14]. The amplified PCR products were analyzed by 1% agarose gel electrophoresis and further purified by Axygen DNA Gel extraction kit. Then ligate the PCR products to the expression vector. The pET SUMO vector and pET-32a vector harbor a His_6-SUMO and His_6-TrxA tag at the N-terminus, respectively. The His_6 tag is helpful for removing the tag proteins and ULP enzyme from the target proteins. In addition, we added a stop codon at the 3′ terminal of the DNA sequence to obtain the natural target protein. The positive clones were further verified by restriction enzyme digestion. The target bands cut from the recombinant plasmid were consistent with the expected fragment size and position. The fragment size was determined as 381 bp for 1–127 domain, 543 bp for 128–309 domain and 309 bp for UBL domain (Fig. 2B). After plasmids were sequenced correctly, the plasmids harboring the target proteins separately with the plasmid containing ULP enzyme were co-transformed into BL21(DE3) competent cells for overexpression of the target protein.

3.2. Expression of the target protein

For the prokaryotic expression system, many factors affect protein expression. Induction temperature is one of the most important factors, especially for proteins that are poorly soluble and easy to accumulate and precipitate. To explore the optimal expression conditions, 5 ml of

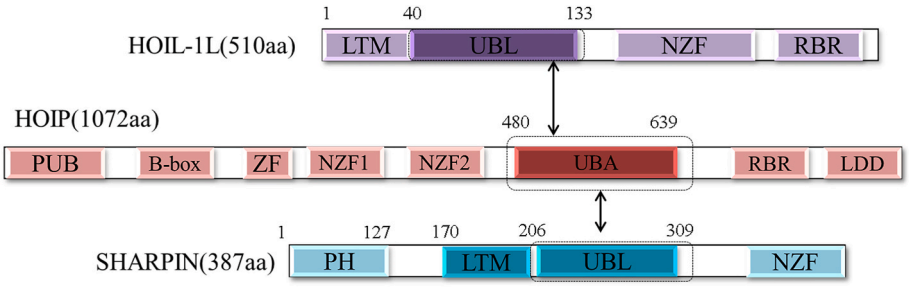

Fig. 1. Schematic representation of the domains of HOIP, SHARPIN and HOIL-1L. The arrow indicates the mutual binding domain between them.

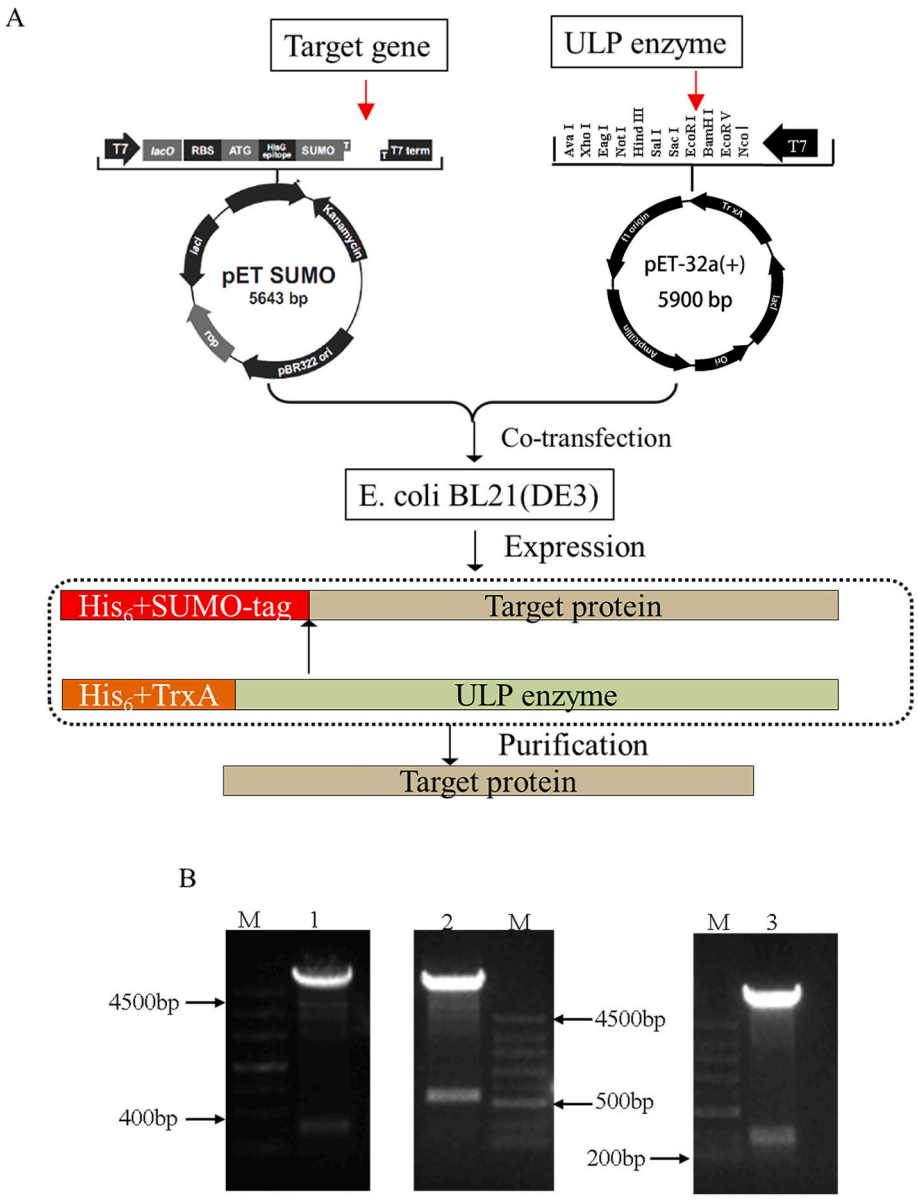

Fig. 2. Construction of co-expression system and Agarose gel electrophoresis analysis after restriction endonuclease cleavage. (A) Co-expression system construction. The target genes include 1–127 domain, 128–309 domain, UBL domain of SHARPIN. (B) Agarose gel electrophoresis analysis after restriction endonuclease cleavage. Lane M, molecular mass marker; Lane 1, 1–127 domain; Lane 2, 128–309 domain; Lane 3, UBL domain.

overnight culture medium was added with 0.5 mm IPTG to induce the expression of the target protein at different temperatures. The expression results were analyzed by SDS-PAGE. The results showed that the constructs of the 1–127 domain and 128–309 domain were highly expressed in the supernatant after incubating for 4 h at 37 °C (Fig. 3A and B). However, the UBL domain yield was high in the supernatant, which was cultured at 16 °C for 24 h (Fig. 3C). The samples of HOIP UBA domain and HOIL-1L$^{1\text{-}140}$ domain have been obtained in previous studies [14]. Since the sizes of 1–127 domain and SUMO tag were basically same, no two protein bands were observed in the expression result (Fig. 3A). But the 1–127 domain could be separated from SUMO tag and high yield of 1–127 domain could be obtained in the purification process, indicating that the SUMO tag could be completely cut off and separated from the target proteins by this expression system (Fig. 3). These results further proved that this method could be considered for the soluble expression of most recombinant proteins.

3.3. Purification of target protein

According to the results of small amount expression of the target protein, the large amount of the target protein was expressed under the same conditions. The advantage of using co-expression system as mentioned above was that the SUMO tag was completely digested in the expression process, which could reduce the steps of purification [14]. Briefly, for purification of 1–127 domain, 128–309 domain, and UBL domain of SHARPIN, the supernatant was purified by Ni-NTA affinity column equilibrated with buffer A. The captured column was washed with buffer A and then eluted with 10, 20, and 40 mM imidazole buffers to collect the target proteins. The SUMO-tag and ULP enzyme containing the His_6 tag were eluted with 250 mM imidazole buffer. The fractions of 10, 20, and 40 mM imidazole elution were combined together and loaded onto Superdex 200 column for further purification and buffer exchange. The SDS-PAGE results showed that the purity of the target proteins was higher than 95%. The gel filtration chromatography results also showed that all the target proteins existed in homogeneous

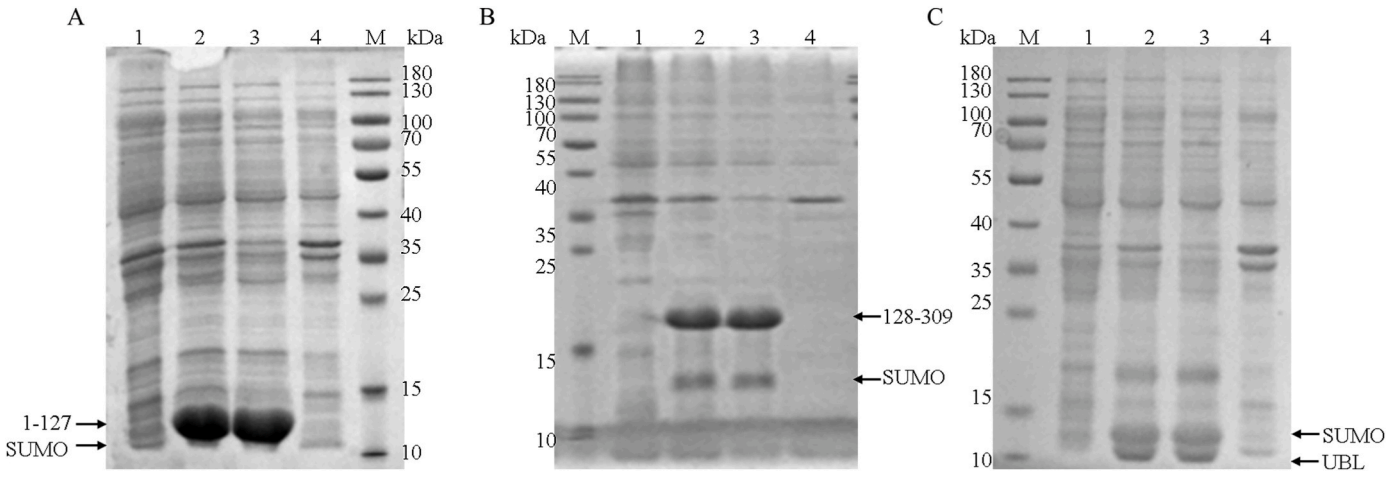

Fig. 3. The test expression results. (A) Test expression results of 1–127 domain; (B) Test expression results of 128–309 domain; (C) Test expression results of UBL domain. Lane M, molecular mass marker; lane 1, lysate of whole cells before IPTG induction; lane 2, lysate of whole cells after induction; lane 3, the supernatant fraction; lane 4, precipitate from the lysate. The arrows indicate the expression of the target proteins.

monomers. In addition, their positions in SDS-PAGE bands were also consistent with the theoretical relative molecular weight (Fig. 4). The yield of target protein per liter of bacterial culture was about 40 mg–50 mg. They also were very stable and without degradation and aggregation when stored in the refrigerator for several weeks or at room temperature for one month. In addition, the purified protein could be concentrated to 20 mg/ml without precipitation. Another advantage of this method is that the target proteins don't contain the His_6 tag.

3.4. Secondary structure analysis

The secondary structure of the target protein was analyzed by CD spectrum to analyze the difference in the secondary structure of each domain of SHARPIN. From the results, the far-UV CD spectra of these target domain were similar. They all showed a negative maximum peak at 208 nm, indicating that the secondary structure of the target protein was rich in α-helix. In addition, two negative peaks were also observed at about 205 nm and 219 nm, indicating that the secondary structure of these target proteins also contains β-sheet (Fig. 5). The CDNN software was used to analyze the secondary structure content of target proteins based on the far-UV CD spectra. The content of α-helix and β-sheet were summarized in Table 1 and β-sheet occupied the main component. These results were consistent with previous reports, indicating that the target protein prepared according to our strategy could fold correctly [12,15].

3.5. Structural stability determination

The difference of stability between the 1–127 domain, 128–309 domain and UBL domain was detected by thermal-induced and urea-induced unfolding experiments. CD spectroscopy was also used to investigate the structural changes during the unfolding process of the target domain. The unfolded protein fraction was represented by the unfolded fraction F_{un} calculated according to reference [16]. Similarly, by measuring the CD value at 222 nm with different temperatures and urea concentrations, the transition curves of thermal-induced and urea-induced target protein unfolding were obtained. The secondary structure loss process and transition midpoint (T_m and C_m) induced by thermal and urea could be observed from the transition curve (Fig. 6). The range of secondary structure loss, T_m and C_m values of the target protein were summarized in Table 2. With the increase of temperature and urea concentration, the secondary structure of protein gradually decreased and ultimately disappeared. The results showed that the structural stability of the 128–309 domain was higher than the UBL domain, indicating that the existence of the N-terminal UBL domain made the overall structure more stable than the alone UBL domain. In addition, the structural stability of 1–127 domain was higher than the 128–309 domain and UBL domain, indicating that 1–127 domain adopted a more stable conformation.

3.6. Biological activity determination of target protein

Since the prokaryotic expression system lacks post-translational modification, most of the expressed target protein is inactive. In this study, we used HOIP UBA domain and HOIL-1L$^{1\text{-}140}$ domain as the ligands to interact with each fragment of SHARPIN to determine their binding ability and whether the target proteins prepared by co-

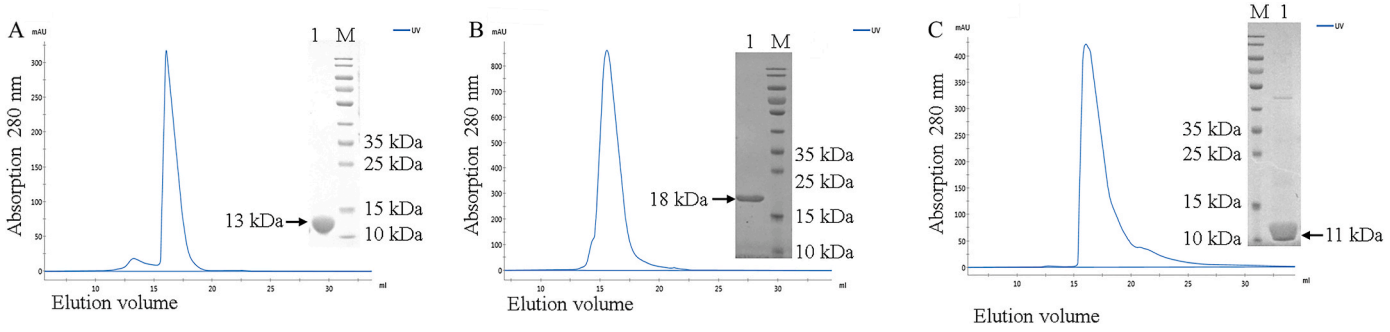

Fig. 4. Gel filtration chromatogram and SDS-PAGE analysis after purification of the target protein. (A) Purification results of 1–127 domain; (B) Purification results of 128–309 domain; (C) Purification results of UBL domain. Lane M, molecular mass marker; Lane 1, SDS-PAGE analysis of target proteins. The arrows indicate the purification of the target proteins.

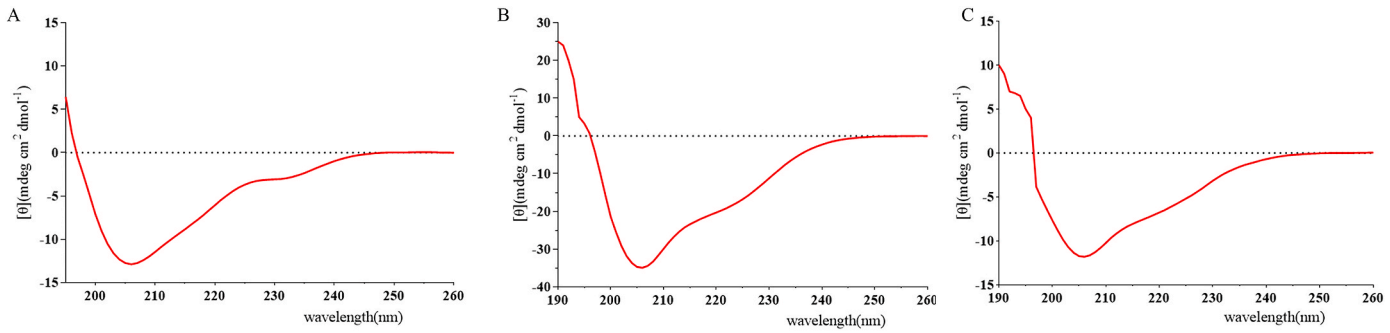

Fig. 5. CD characterization of target proteins. The secondary structure elements of target proteins were characterized by far-UV CD spectroscopy with wavelength range from 190 to 250 nm. (A) Far-UV CD spectra of 1–127 domain recorded at 25 °C; (B) Far-UV CD spectra of 128–309 domain recorded at 25 °C; (C) Far-UV CD spectra of UBL domain recorded at 25 °C.

Table 1
CD characterization of target proteins.

	Secondary elements (%)		
	α-Helix	β-Sheet	Coil
1-127 domain	26.9	55	28.1
128-309 domain	19.4	51.3	29.3
UBL domain	13.4	56.2	30.4

expression had the biological activity. The purified UBA and HOIL-1L$^{1\text{-}140}$ domain were separately incubated with 1–127 domain, 128–309 domain, and UBL domain of SHARPIN at 1:1 M ratio, respectively, at room temperature for 1 h, and followed by analytical gel filtration chromatography and SDS-PAGE analysis. The results showed that the absorbance peak at 280 nm (A280) became higher, and the occurrence time of the complex peak was earlier when the UBA was combined with 128–309 domain or UBL domain. The corresponding SDS-PAGE results also confirmed that both 128–309 domain and UBL domain could interact with UBA domain to form binary complexes (Fig. 7B and C). In contrast, there was no significant change in the occurrence time and height of complex peak after incubation of 1–127 domain with UBA domain. There was another peak after the UBA absorption peak (Fig. 7A).

On the other hand, when the HOIL-1L$^{1\text{-}140}$ was incubated with each fragment of SHARPIN, the results showed that only the A280 of the complex peak became much higher, and the complex peak was eluted earlier when combined with 128–309 domain. After incubated with 1–127 domain or UBL domain of SHARPIN, the position of the absorption peak did not change significantly, and there was another peak after the HOIL-1L$^{1\text{-}140}$ domain absorption peak (Fig. 7D, E, F). These results further confirmed that the interaction between the UBL domain of SHARPIN and the UBA domain of HOIP was involved in the formation of LUBAC. In addition, this result also proved that SHARPIN interacted with HOIL-1L through the 128–309 domain to form a complex.

3.7. Evaluation of binding affinity

Furthermore, kinetic studies were performed to determine the difference of binding affinity of UBA domain with 128–309 domain, UBL domain, and 128–309 domain/HOIL-1L$^{1\text{-}140}$ complex domain, respectively. The HOIL-1L$^{1\text{-}140}$ domain, the 128–309 domain, and UBL domain of SHARPIN concentrations ranged from 20 μM to 1 μM (Fig. 8). The on-rate kinetic (K_{on}) values were displayed by 128–309 domain at *3.25 E* +03 Ms^{-1}, UBL domain at *2.85 E* +02 Ms^{-1}, and 128–309 domain/HOIL-1L$^{1\text{-}140}$ domain complex at *5.34 E* +04 Ms^{-1}. The off-rate kinetic (K_{off}) values were displayed by 128–309 domain at *6.55 E* -04 M^{-1}, UBL domain at *5.45 E* -03 M^{-1}, and 128–309 domain/HOIL-1L$^{1\text{-}140}$ domain complex at 3.37 *E* -06 M^{-1}. The equilibrium dissociation constant (K_D) was calculated by K_{off}/K_{on} to analyze the difference of binding affinity. The results showed that the UBA domain had a strong affinity to the 128–309 domain than the UBL domain, with the K_D values of *2.015 E -07 M* and *1.912 E -05 M*, respectively. However, when the complex of 128–309 domain/HOIL-1L$^{1\text{-}140}$ domain was titrated with UBA domain, the affinity became stronger compared to the alone 128–309 domain with the K_D value of *6.311 E* -11 M^{-1} (Fig. 8A, B, C). The K_{on}, K_{off} and K_D values of the 128–309 domain to HOIL-1L$^{1\text{-}140}$ were *4.17 E* +03 Ms^{-1}, *5.28 E* -05 M^{-1}and *1.266 E* -07 M^{-1}, respectively, indicating that 128–309 domain also had a strong affinity for HOIL-1L$^{1\text{-}140}$ domain (Fig. 8D). The results indicated that the existence of the N-terminal UBL domain strengthened the binding ability of the UBL domain with the UBA domain and made their combination more stable. However, when 128–309 domain and HOIL-1L$^{1\text{-}140}$ domain coexisted, the ternary

Table 2
Unfolding parameters of 128–309 domain and UBL domain.

	Thermal unfolding (°C)	Urea-induced unfolding (mol/L)
	Transition range T_m	Transition range C_m
1-127 domain	47.2–75.0 55.2	2.75–6.00 3.500
128-309 domain	41.2–73.0 51.3	2.25–5.50 3.125
UBL domain	33.2–67.0 49.1	1.50–4.25 2.625

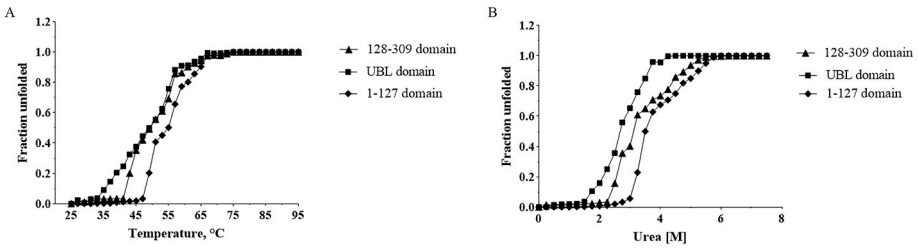

Fig. 6. Thermal-induced and Urea-induced unfolding transitions of 1–127 domain, 128–309 domain and UBL domain were measured by CD ellipticity at 222 nm. (A) Thermal unfolding recorded from 25 to 95 °C; (B) The urea-induced unfolding was recorded at 25 °C.

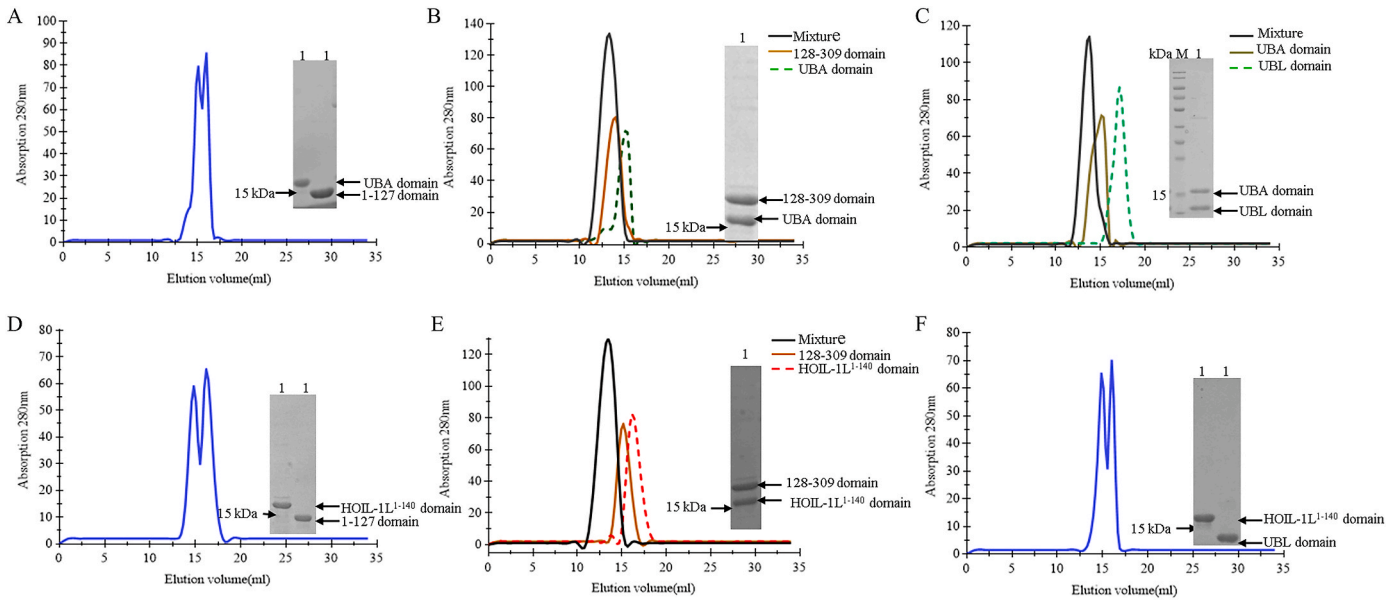

Fig. 7. Analysis of bioactivity of target proteins by gel filtration chromatography combined with SDS-PAGE. (A) Determination of interaction between UBA domain and 1–127 domain; (B) Determination of interaction between UBA domain and 128–309 domain; (C) Determination of interaction between UBA domain and UBL domain. (D) Determination of interaction between 1 and 127 domain and HOIL-1L$^{1\text{-}140}$ domain. (E) Determination of interaction between 128 and 309 domain and HOIL-1L$^{1\text{-}140}$ domain. (F) Determination of interaction between UBL domain and HOIL-1L$^{1\text{-}140}$ domain. Lane M, molecular mass marker; Lane 1, the protein components of the corresponding fraction.

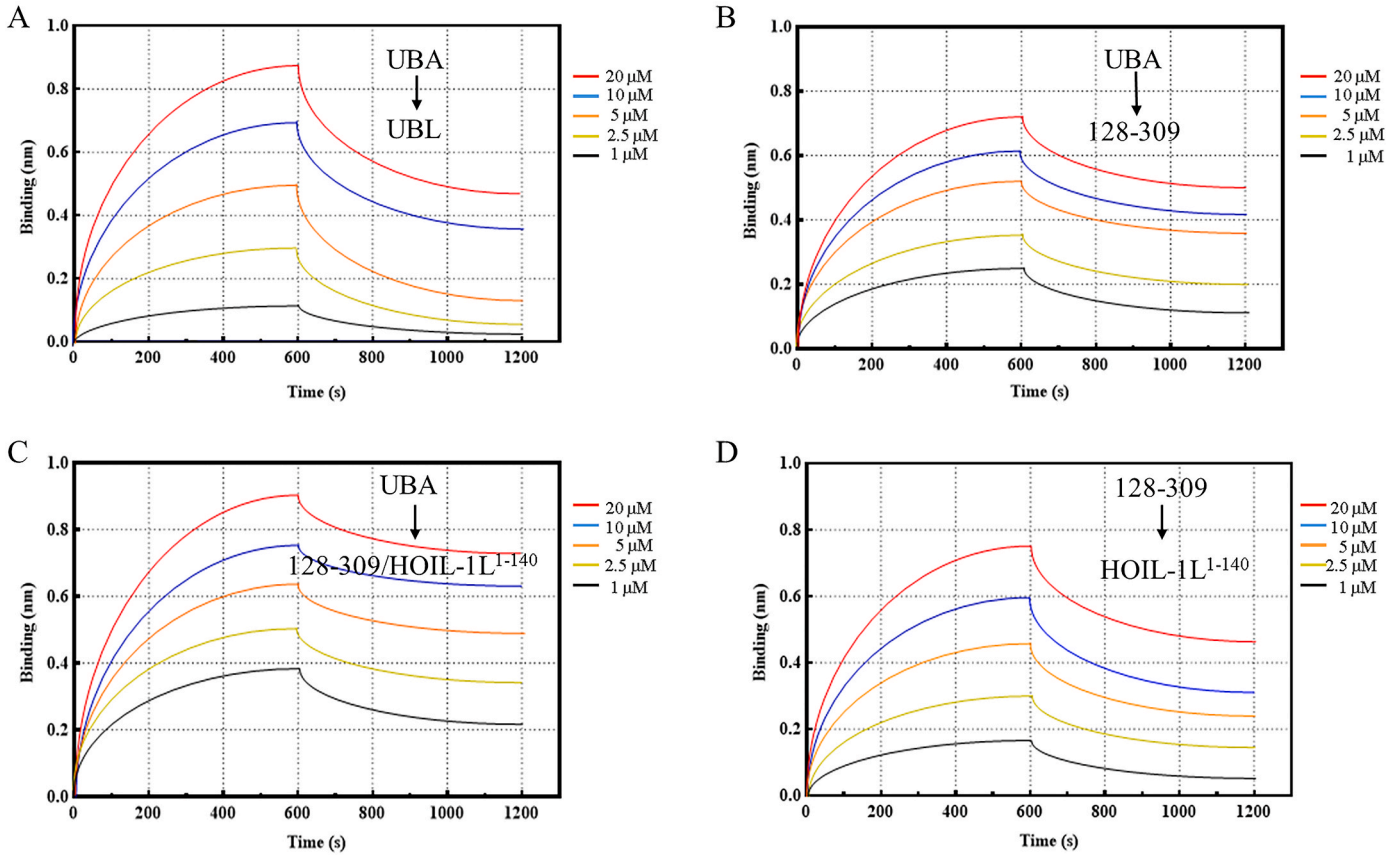

Fig. 8. Binding affinity measurements via the biosensor experiments. (A) UBA domain to UBL domain; (B) UBA domain to 128–309 domain. (C) UBA domain to 128–309 domain/HOIL-1L$^{1\text{-}140}$ domain complex. (D) 128–309 domain to HOIL-1L$^{1\text{-}140}$ domain. Curves correspond to the phases of association and dissociation of 128–309 domain, UBL domain and HOIL-1L$^{1\text{-}140}$ domain at various concentrations on the UBA domain anchored to the sensor chip. These curves may be used to determine the K_D, K_{on}, and K_{off}.

complexes with UBA domain were more stable than 128–309 domain alone.

4. Discussion

SHARPIN, not only a key component of LUBAC participates in regulating the activation of NF-κB in innate immunity, but also can inhibit β_1-integrin activation [17,18]. SHARPIN participates in the formation of LUBAC and inhibits the activation of integrin through the UBL domain [19]. But the role of the N-terminal UBL domain of SHARPIN still remains elusive. In order to obtain a sufficient number of stable and active protein samples to clarify the detailed biochemical characteristics of UBL N-terminal domain of SHARPIN, we truncated the domain before NZF of SHARPIN to 1–127 domain, 128–309 domain, and UBL domain respectively. However, the UBL domain and 128–309 domain are rich in multiple disulfide bonds and contain multiple isolated cysteines. For their recombinant expression and purification, before we had tried a variety of expression conditions and multiple expression vectors, but we had not obtained the target protein that could be used for structural and functional research. For example, inclusion bodies were easy to form during expression, or aggregation and precipitation due to the instability of the target protein in the purification process [20]. On the basis of successfully obtaining UBA domain of HOIP and UBL domain of HOIL-1L by the SUMO co-expression system, we used the same method for 1–127 domain, 128–309 domain, UBL domain of SHARPIN expression [14]. Finally, we successfully obtained stable and biologically active protein samples for biochemical characterization.

Proteins often undergo conformational changes to execute their biological functions, such as an enzyme reaction or ligand binding [21]. The correct folding of target protein conformations is helpful to perform their biological functions. However, achieving effective protein folding, disulfide bond formation, and post-translational modification in *E. coli* are very difficult [22]. To examine whether the proteins produced by the co-expression system were folded correctly and had biological activity, we analyzed the secondary structure of target protein by CD spectroscopy, and then analyzed the relationship between SHARPIN and HOIP, HOIL-1L by analytical gel filtration chromatography. The CD spectrum recorded on the 1–127 domain, 128–309 domain and UBL domain of SHARPIN described in this work were consistent with the previously reported natural or recombinant proteins. These results indicated that all the target proteins prepared according to our strategy could fold correctly, although these proteins lacked natural post-translational modifications due to their expression in prokaryotic hosts [12,15]. The secondary structure contents of four proteins were also consistent with those previously reported. They were all proteins with β-sheet as the main feature.

In addition, we also used CD experiment to analyze the difference in stability between 1 and 127 domain, 128–309 domain, and UBL domain. The results showed that the stability of the 128–309 domain was higher than the UBL domain. These results showed that the existence of the N-terminal UBL domain could increase the stability of the overall structure and made the overall structure more compact than the single UBL domain. However, the structural stability of 1–127 domain was higher than 128–309 domain and UBL domain. Previous studies have shown that the 1–127 domain adopted the PH domain superfold and had the characteristics of the concentration-dependent monomer-dimer balance [12]. Therefore, our results showed that the 1–127 domain existed in the form of monomer at low concentration and had high structural stability.

Then we analyzed whether the target proteins prepared in this experiment could be used for functional research and which fragment of SHARPIN was involved in the formation and stability of LUBAC. Previous studies have shown that the 1–127 domain of SHARPIN wasn't used as a protein-ligand interaction platform, but as a scaffold to provide a structural basis for homo-dimerization under *in vitro* conditions. The UBL domain was combined with the UBA domain of HOIP to participate in the formation of LUBAC [4,12,19,23,24]. The results of analytical gel filtration chromatography and following SDS-PAGE proved that SHARPIN could bind to the UBA domain of HOIP only if it contained UBL domain. In addition, SHARPIN could also participate in the stabilization of LUBAC through the interaction between 128 and 309 domain and HOIL-1L$^{1\text{-}140}$ domain. These results also confirmed that the target protein prepared according to the co-expression strategy had biological activity and could be used for functional research.

Finally, we analyzed the difference of binding ability between UBA domain with 128–309 domain, UBL domain, and 128–309 domain/HOIL-1L$^{1\text{-}140}$ domain complex by Octet RED96 system. Interestingly, the binding ability and anti-dissociation ability of the 128–309 domain to UBA domain was higher than the UBL domain, and the affinity of UBA domain to 128–309 domain/HOIL-1L$^{1\text{-}140}$ domain complex was higher than that of 128–309 domain alone. Previous studies have shown that the N-terminal UBL domain of SHARPIN and HOIL-1L folded into a single spherical domain to resist dissociation and played a key role in stabilizing trimer LUBAC [4,25]. Our results also showed that the presence of the N-terminal UBL domain of SHARPIN alone also could enhance the binding and resist dissociation ability of the UBA domain and UBL domain (Fig. 9), which have not been reported in previous studies. We tried to solve the structure of the 128–309 domain and UBA domain complex by X-ray crystallography that could clarify the mechanism of the 128–309 domain enhancing the binding ability and resisting dissociation ability. Furthermore, X-ray crystallography and NMR titration experiments will be used to determine the complex crystal structures and explore how the UBL N-terminal domain of SHARPIN enhances the binding ability with UBA domain of HOIP.

5. Conclusions

In this experiment, we constructed the 1–127 domain, 128–309 domain, and UBL domain of SHARPIN expression vectors through genetic engineering technology. Optimized protein expression and purification conditions, high purity, high yield, and stable target proteins were obtained by co-expression method. Finally, the interaction between 1 and 127 domain, 128–309 domain, UBL domain of SHARPIN with UBA domain of HOIP and HOIL-1L$^{1\text{-}140}$ domain were analyzed, and the secondary structure components of 1–127 domain, 128–309 domain and UBL domain were determined by CD spectroscopy. In addition, both thermal-induced and urea-induced unfolding results demonstrated that the existence of the N-terminal UBL domain could make the overall structure more stable than the alone UBL domain. Finally, biosensor experiments showed that the existence of a separate N-terminal UBL domain could also enhance the combination ability of the UBL domain and the UBA domain. These results were conducive to the further study of the structure and function of SHARPIN.

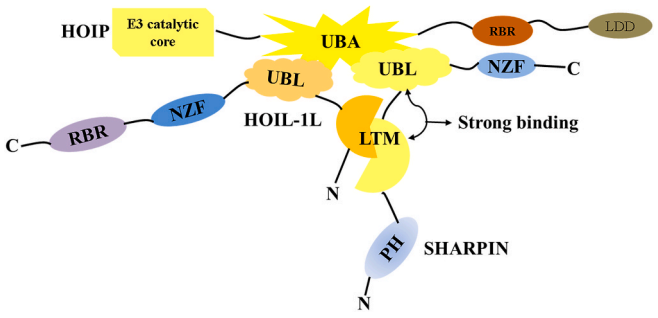

Fig. 9. Mechanism of stability and formation of trimer LUBAC. SHARPIN and HOIL-1L aggregate on HOIP through rapid interaction between UBL domain and UBA domain. In this process, the LTM domain of the SHARPIN and HOIL-1L could enhance their binding ability to HOIP.

Ethics approval and consent to participate

Not applicable.

Consent for publication

All authors give consent to publish the research in Protein Expression and Purification.

Availability of data and materials

The datasets and material used during this study are available from the corresponding author.

Funding information

This work was supported by the grant from the Heilongjiang Key Laboratory for Laboratory Animals and Comparative Medicine (No.518001), and National Natural Science Foundation of China (No. 32071120).

CRediT authorship contribution statement

Wenlei Ma: designed the research, performed most experiments and prepared the manuscript. **Ying Lu:** did the data analysis. **Jing Qi:** did the data analysis. **Yongmei Zuo:** did the data analysis. **Chenchen Wang:** did the data analysis, and. **Xiaodong Zheng:** revised the manuscript. All authors read and approved the final manuscript. **Jiafu Liu:** designed the research, revised the manuscript. All authors read and approved the final manuscript.

Declaration of competing interest

The authors declare that they have no competing interests.

Acknowledgments

Not applicable.

References

[1] S. Lim, C. Sala, J. Yoon, S. Park, S. Kuroda, M. Sheng, et al., Sharpin, a novel postsynaptic density protein that directly interacts with the shank family of proteins, Mol. Cell. Neurosci. 17 (2) (2001) 385–397.
[2] C.S. Potter, Z. Wang, K.A. Silva, V.E. Kennedy, T.M. Stearns, L. Burzenski, et al., Chronic proliferative dermatitis in Sharpin null mice: development of an autoinflammatory disease in the absence of B and T lymphocytes and IL4/IL13 signaling, PLoS One 9 (1) (2014), e85666.
[3] K. Sasaki, K. Iwai, Roles of linear ubiquitinylation, a crucial regulator of NF-κB and cell death, in the immune system, Immunol. Rev. 266 (1) (2015) 175–189.
[4] H. Fujita, A. Tokunaga, S. Shimizu, A.L. Whiting, F. Aguilar-Alonso, K. Takagi, et al., Cooperative domain formation by homologous motifs in HOIL-1L and SHARPIN plays A crucial role in LUBAC stabilization, Cell Rep. 23 (4) (2018) 1192–1204.
[5] B. Boisson, E. Laplantine, C. Prando, S. Giliani, E. Israelsson, Z. Xu, et al., Immunodeficiency, autoinflammation and amylopectinosis in humans with inherited HOIL-1 and LUBAC deficiency, Nat. Immunol. 13 (12) (2012) 1178–1186.
[6] N. Peltzer, E. Rieser, L. Taraborrelli, P. Draber, M. Darding, B. Pernaute, et al., HOIP deficiency causes embryonic lethality by aberrant TNFR1-mediated endothelial cell death, Cell Rep. 9 (1) (2014) 153–165.
[7] J. Gao, Y. Bao, S. Ge, P. Sun, J. Sun, J. Liu, et al., Sharpin suppresses β1-integrin activation by complexing with the β1 tail and kindlin-1, Cell Commun. Signal. 17 (1) (2019).
[8] A. Kasirer-Friede, W. Tjahjono, K. Eto, S.J. Shattil, SHARPIN at the nexus of integrin, immune, and inflammatory signaling in human platelets, Proc. Natl. Acad. Sci. U.S.A. 116 (11) (2019) 4983–4988.
[9] F. Tokunaga, S.I. Sakata, Y. Saeki, Y. Satomi, K. Iwai, Involvement of linear polyubiquitylation of NEMO in NF-B activation, Nat. Cell Biol. 11 (2) (2009) 123–132.
[10] D. Gullberg, N. De Franceschi, E. Peuhu, M. Parsons, S. Rissanen, I. Vattulainen, et al., Mutually exclusive roles of SHARPIN in integrin inactivation and NF-κB signaling, PLoS One 10 (11) (2015).
[11] F. Tokunaga, T. Nakagawa, M. Nakahara, Y. Saeki, M. Taniguchi, S.I. Sakata, et al., SHARPIN is a component of the NF-κB-activating linear ubiquitin chain assembly complex, Nature 471 (7340) (2011) 633–636.
[12] B. Stieglitz, L.F. Haire, I. Dikic, K. Rittinger, Structural analysis of SHARPIN, a subunit of a large multi-protein E3 ubiquitin ligase, reveals a novel dimerization function for the pleckstrin homology superfold, J. Biol. Chem. 287 (25) (2012) 20823–20829.
[13] J.J. Smit, D. Monteferrario, S.M. Noordermeer, W.J. Van Dijk, dR. Van, A. Bert, T. K. Sixma, The E3 ligase HOIP specifies linear ubiquitin chain assembly through its RING-IBR-RING domain and the unique LDD extension, EMBO J. 31 (19) (2012) 3833–3844.
[14] W. Ma, Y. Lu, Y. Zuo, C. Wang, J. Liu, Effects of Removing a Highly Conserved Disulfide Bond in Ubiquitin-Associated Domain of Human HOIP on Biochemical Characteristics, Protein Expression and Purification, 2022, p. 190.
[15] J. Liu, Y. Wang, Y. Gong, F. Tao, L. Pan, Structural insights into SHARPIN-mediated activation of HOIP for the linear ubiquitin chain assembly, Cell Rep. 21 (1) (2017) 27–36.
[16] C. Guo, Y. Lian, Q. Liu, J. Liu, Y. Zhang, D. Lin, Soluble expression and characterization of a mouse epididymis-specific protein lipocalin6, Protein Expr. Purif. 69 (1) (2010) 64–67.
[17] K. Iwai, F. Tokunaga, Linear polyubiquitination: a new regulator of NF-kappaB activation, EMBO Rep. 10 (7) (2009) 706–713.
[18] J.K. Rantala, J. Pouwels, T. Pellinen, S. Veltel, P. Laasola, E. Mattila, et al., SHARPIN is an endogenous inhibitor of β1-integrin activation, Nat. Cell Biol. 13 (11) (2011) 1315–1324.
[19] N.D. Franceschi, E. Peuhu, M. Parsons, S. Rissanen, I. Vattulainen, M. Salmi, et al., Mutually exclusive roles of SHARPIN in integrin inactivation and NF-κB signaling, PLoS One 10 (11) (2015) 1–16, https://doi.org/10.1371/journal.pone.0143423.
[20] Y. Peng, J. Liu, Q. Liu, Y. Yao, C. Guo, Y. Zhang, et al., Conformational and biochemical characterization of a rat epididymis-specific lipocalin 12 expressed in Escherichia coli, Biochim. Biophys. Acta Protein Proteonomics 1804 (11) (2010) 2102–2110.
[21] J. Liu, C. Guo, Y. Yao, D. Lin, Effects of removing a conserved disulfide bond on the biological characteristics of rat lipocalin-type prostaglandin D synthase, Biochimie 90 (11–12) (2008) 1637–1646.
[22] K. Peciak, R. Tommasi, J.W. Choi, S. Brocchini, E. Laurine, Expression of soluble and active interferon consensus in SUMO fusion expression system in E. coli, Protein Expr. Purif. 99 (2014) 18–26.
[23] Kasirer-Friede Ana, Tjahjono Winson, Eto Koji, et al., SHARPIN at the Nexus of Integrin, Immune, and Inflammatory Signaling in Human Platelets, Proceedings of the National Academy of Sciences of the United States of America, 2019.
[24] B. Stieglitz, R.R. Rana, M.G. Koliopoulos, A.C. Morris-Davies, V. Schaeffer, E. Christodoulou, et al., Structural basis for ligase-specific conjugation of linear ubiquitin chains by HOIP, Nature 503 (7476) (2013) 422–426.
[25] E. Walinda, D. Morimoto, T. Sorada, K. Iwai, K. Sugase, Expression, solubility monitoring, and purification of the co-folded LUBAC LTM domain by structure-guided tandem folding in autoinducing cultures, Protein Expr. Purif. 187 (2021) 105953.